4 A Brush-Forming PAA with a Capping Domain*

(* contains material reprinted from Ref. 1 with permission from the American Chemical Society)

4.1 Background for Journal Article

During our research, we became interested in investigating the surface adsorption characteristics of a PAA consisting of: an anchor block, a linker region and a 'capping domain'. The capping domain is defined as a globular protein with a defined tertiary structure. These types of polymers would be useful in brush-forming applications such as in biomaterials research where they might be useful serving as specialty coatings (*i.e.* anti-thrombic, antibiotic, or cell-attachment promoting coatings). We decided that the Trx-$Pro_{39}Glu_{10}$ product (from Chapter 3) would act as a convenient model for this system where the proline block serves as a linker that tethers a folded protein (Trx) to the adsorbing acidic anchor block. Here, the HP-Thioredoxin not only aids in the expression, purification and detection of the PAA product, but it is also an integral part of the surface-active PAA. Section 4.1.1 discusses why HP-Thioredoxin works as a model capping domain.

A series of solution and surface adsorption studies were conducted using the Trx-$Pro_{39}Glu_{10}$ product by students in Dr. Richey M. Davis' and Dr. William A. Ducker's research groups. The work was recently accepted for publication in *Langmuir* and is presented in Section 4.2. In the article, we show that our Trx-$Pro_{39}Glu_{10}$ product successfully forms sufficient brush layers on aluminum oxide surfaces for colloidal stabilization applications.

4.1.1 HP-Thioredoxin as a Capping Domain

Figure 4.1 shows a schematic of a surface-active PAA containing a Trx protein as its capping domain. Prior to our studies, there were several indications that Trx would serve as a suitable capping domain. Trx is a protein with a molecular weight of ~12 kDa and is extremely soluble in aqueous solutions. This is beneficial since in order for the capping domain to retain its tertiary structure it must remain in solution.

[1] Tulpar A, Henderson DB, Mao M, Caba B, Davis RM, Van Cott KE and Ducker WA. "Unnatural proteins for the control of surface forces". *Langmuir*. (in print).

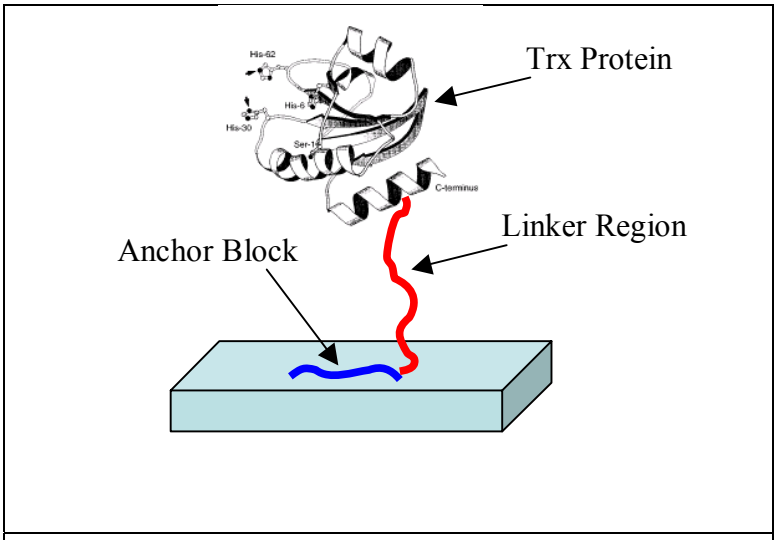

Figure 4.1. Schematic of surface-active PAA with a folded protein as a capping domain.

The capping domain also must not adsorb onto the surface. Using the pK_a values of the ionizable amino acids within the Trx domain, the net charge on Trx as a function of pH was calculated. This relationship is shown in Figure 4.2. The isoelectric point (IEP) of the capping domain is ~6.3. For pH's slightly above the IEP (pH 6.3-8), the Trx has a slightly negative charge. However, this charge is so small that Trx should not compete with a highly negatively charged acidic anchor block for adsorption onto a positively charged surface, such as alumina. For pH's slightly below the IEP (pH 5-6.3), the Trx has a slightly positive charge. Therefore, under these conditions, we expect there to be an electrostatic repulsion between the capping domain and alumina surface. Hence, we hypothesize that in the pH range of 5-8, Trx should serve as an ideal capping domain for a surface-active polymer that forms brush layers on alumina.

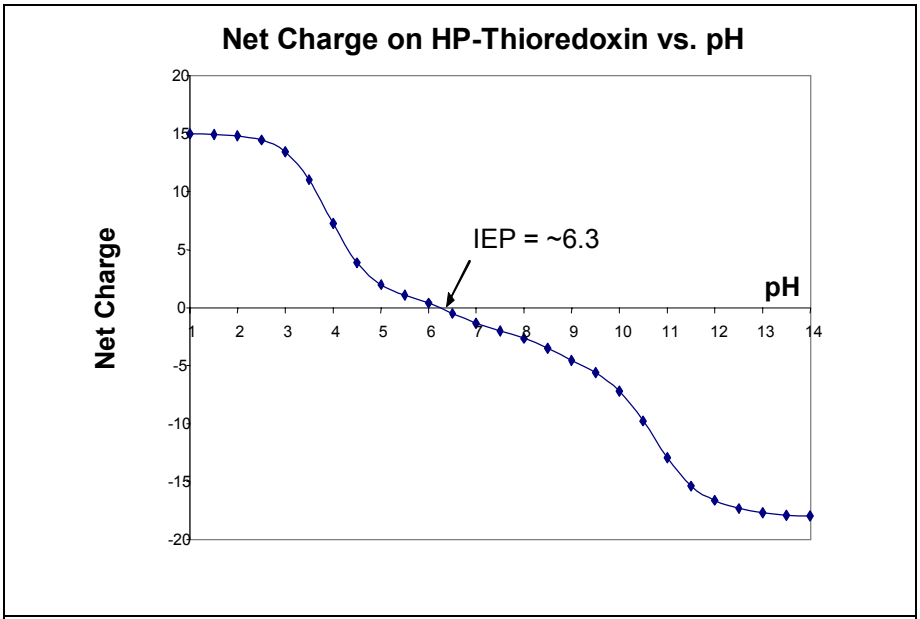

Figure 4.2 Calculated net charge on Trx as a function of pH.

Reprinted from Tulpar A, Henderson DB, Mao M, Caba B, Davis RM, Van Cott KE and Ducker WA. *Langmuir* (in print), with permission from the American Chemical Society.

4.2 Journal Article: "Unnatural Proteins for the Control of Surface Forces"

Aysen Tulpar[a], Douglas B. Henderson[b], Min Mao[a], Beth Caba[b], Richey M. Davis[b], Kevin E. Van Cott[b] and William A. Ducker[a].

[a] Department of Chemistry, Virginia Tech, Blacksburg, Virginia 24061, USA
[b] Department of Chemical Engineering, Virginia Tech, Blacksburg, Virginia 24061, USA

4.2.1 Abstract

We introduce a new method for the stabilization of colloidal particles via the synthesis and adsorption of unnatural proteins. Biosynthesis of protein-based polymers offers the advantages of the preparation of complex sequences through control of the primary sequence, monodisperse polymers, ease of combinatorial search for anchor blocks, environmentally-friendly synthesis, use of water as the solvent, and incorporation of a palette of known natural proteins. We have synthesized an unnatural protein with the sequence: (HP-Thioredoxin)-$Pro_{39}Glu_{10}$ for modification of the forces between alumina particles. The polyglutamate sequence, Glu_{10}, is anionic (pH > 3) and is designed to anchor the protein to positively charged solids, *e.g.* alumina in water (pH <9). The polyproline sequence, Pro_{39}, is neutral. The thioredoxin is a recombinant from of the natural globular protein with a histidine patch (HisPatch-Thioredoxin or Trx), and is zwitterionic. The combined Trx-Pro_{39} sequence is hydrophilic with pI ~ 6.3. This block is designed to remain in solution, thereby providing a steric barrier to the approach of two particles in a range of salt and pH conditions. Ellipsometry experiments show that Trx-$Pro_{39}Glu_{10}$ does adsorb to alumina. Force measurements with the Atomic Force Microscopy (AFM) colloid probe technique show that adsorption of the fusion protein leads to repulsive forces that decay exponentially with the separation between the surfaces, and are independent of salt concentration in the range 0.001–0.1 M KNO_3. This demonstrates that the repulsive forces are not electrostatic. We hypothesize that the repulsion is due to confinement and loss of solvent for the adsorbed polymer; the forces are similar to those expected for a polymer brush. Force measurements between Trx-coated alumina surfaces also show a repulsive force, but the force has a decay length that is consistent with electrostatic double-layer forces: the Trx has not neutralized the surface charge of the underlying alumina.

Our results point to interesting future experiments where recombinant DNA technology could be used to synthesize fusion proteins containing useful natural proteins and an anchor. This may allow preparation, via single-step aqueous self assembly, of anchored proteins that maintain their natural structure. Our technique is not limited to homopolymer blocks; more complex primary sequences can be used.

4.2.2 Introduction

Many items are fabricated from a dense suspension of colloidal particles that is formed into the desired shape, pressurized, and then sintered to increase the area of contact between the particles. This colloidal processing technique relies on the ability to form a suspension of controlled density and viscosity. For example, in ceramic processing, it is desirable to form a high-density suspension for strength of the fired

ceramic, and low viscosity for ease of molding (workability). Many clay minerals exhibit these properties naturally in water thereby allowing the development of ceramic engineering in the absence of science. To achieve the workability of clay with a different type of particle requires knowledge of the origin of workability, and a means to implement this knowledge.

It is now well known that workability arises from repulsive forces between particles;[1] if the forces are monotonically attractive and strong, then each particle collision results in the particles becoming trapped in an adhesive minimum with a structure that relates to the geometry of the collision, and is not controlled.[2] This produces low density and high viscosity slurries. If the particles exhibit a short-ranged repulsion, then the leading edge of the colliding particles will turn away during the collision and not be immediately trapped in the primary van der Waals minimum.[3, 4] If the particles are not trapped in a deep secondary minimum (<2–5 kT), then the particles can usually slide past each other freely. In fact, a low friction between surfaces has been found to correlate with a low viscosity slurry.[5]

In more advanced applications, it is desirable to go beyond merely imitating the properties of clay and, for example, manipulate the architecture of mixtures of particles or control the orientation of particles. This increased level of control is also achieved through control of the surface forces between the particles.

A van der Waals force will always be present, and is always attractive between like particles. Because the van der Waals force, F, has a power-law dependence ($F = \frac{AR}{12S^2}$ where the objects are spheres of radius, R, S is the separation between the surfaces, and A is the Hamaker constant),[6] the force becomes very large and attractive at small separations. Unfortunately, particle processing is sometimes hindered by the fact that some ceramic particles have a large Hamaker constant in water (*e.g.* $\sim 5\times10^{-20}$ for alumina–water–alumina).[7] The ability to gain control of interparticulate forces is largely a problem of reducing the van der Waals force by immersing the particles in a medium or coating the surface, or overcoming the van der Waals force with another force, such as the electrostatic double-layer force, a hydration force, or a polymer steric force.

Another important consideration in the design of suspensions is the cost and environmental impact of the solvent. Water is the preferred solvent because it has the minimum environmental impact, and it is inexpensive. The high dielectric constant of water suggests that the remedy is a repulsive double-layer force. This solution is undesirable from two aspects; the need to add a large amount of salt, which may remain after firing; and the potential impact of uncontrolled salt in feedwater.

An alternative means of stabilizing particles is to adsorb organic molecules to the surface of the particle. This has two advantages: the adsorbed molecules can generate additional repulsive steric forces, and the adsorption will often reduce the van der Waals force.[8] A very thick dense hydrocarbon layer will cause a reduction of the Hamaker constant to $\sim 0.4\times10^{-20}$,[7] a thick layer of polymer with a very high water content will barely change the van der Waals force between the particles, but will keep them sufficiently separated such that the van der Waals force between the particles is insignificant. Other work has focused on the adsorption of (low molecular weight) surfactants.[5, 9,10,11] Here we will focus on the adsorption of polymers.

There is already considerable prior work on the measurement of forces between polymer coated surfaces.[12] The literature most relevant to our work is the measurement of forces between surfaces coated in polymer brushes. A polymer brush forms when the polymer is anchored to the solid with sufficient density that the extent of the polymer brush normal to the interface, L, is greater than the size of the molecule free in solution.[13,14,15,16] de Gennes has used a scaling argument to determine the energy of interaction between adsorbed brushes.[17] The interaction energy per unit area between two flat solids, E_A, as a function of the separation, S, is *approximately*:

$$E_A = \frac{100L}{\pi S^3} k_B T \exp\left(-\frac{\pi S}{L}\right) \qquad (1)$$

for $0.2< S/L<0.9$. T is the temperature and k_B is the Boltzmann constant.

One method for anchoring the polymer to the interface is to use a block copolymer in which one block, the anchor block, has a strong affinity for the solid surface and the other block, the tail block, has a relatively high affinity for the solvent.[18,19,20,21,22] Claesson has measured forces between hydrophobic mica in water with

the adsorbed diblock poly(butyleneoxide)-b-poly(ethyleneoxide).[23,24] The forces were in approximate agreement with de Gennes' scaling theory. Butt *et al.* measured forces between a silicon nitride AFM tip and an alumina-coated glass slide with the adsorbed diblock poly(methacrylic acid)–b-poly(ethylene oxide) (MAA_6EO_{21}). Before adsorption, the force was attractive, after adsorption the force was repulsive and was fitted to a double-exponential with two decay-lengths: 3.4 and 11.2 nm.[25]

A very similar system was studied by Palmqvist *et al*.[26] They studied the *consolidation* of alumina particles in the presence of the diblock poly(methacrylic acid)–b-poly(ethylene oxide) copolymer and measured the forces between polymer-coated $BaTiO_3$ surfaces. They found that the adsorption of polymer produced a repulsive force on separation of the surfaces.

All of the above experiments studied the adsorption of conventional synthetic polymers. The development of recombinant DNA technologies and recent successes in producing peptide-based polymers, or 'unnatural proteins' (*e.g.* Ref.27,28,29,30,31) suggest a new route to obtaining polymers for the control of particle suspensions. We propose a new strategy in which the colloidal scientist specifies the exact amino acid sequence of a polymer that is required (the target polymer) and that polymer is synthesized by microorganisms using their native protein synthesis machinery. Briefly, the desired amino acid sequence is coded into DNA and inserted into a microorganism (*e.g.* via a plasmid into *Escherichia coli*). The transformed microorganism is grown into large numbers and directed to express the target polymer. Finally, the cells are harvested and the target polymer is purified for its use in colloidal processing. In the future, it may be possible to also harness biological machinery to synthesize novel polymers from other types of natural monomers, *e.g.* carbohydrates or nucleotides.

There are many potential advantages to this biosynthesis of polypeptide-based polymers. In contrast to conventional polymer synthesis, it is possible in principle to exactly specify in advance the type and position of every monomer in the sequence: one can produce sequences with much greater complexity than the usual diblock or triblock synthetic polymers. Because of the precision with which cells express proteins, monodisperse polymers are produced. The entire procedure is environmentally friendly:

the procedure creates no elemental pollution and water is the only solvent used in the synthesis.

The generic protein design is shown schematically in Figure 4.3. Note that the blocks do not need to be homopolymers, and in fact the absence of homopolymer sequences is preferred for ease of expression in microorganisms.

Figure 4.3 Schematic of polymer sequence. J = joint segment, I = identification segment.

We require a block to bind to the surface in preference to the solvent. More precisely, we also want this block to be able to displace the other segments, so that the spacer and active segments are pushed into solution. The binding block can be found either by rational design, armed with knowledge of the surface chemistry of the solid particle, or by a combinatorial search (*e.g.* Ref.32). A soluble, active block should be at the opposite end of the sequence so that it is presented to the solution. In some cases a soluble spacer segment will be required to move the active block away from the solid and to allow extra conformational freedom for the active element. This block would normally be hydrophilic to maintain its partitioning into the solvent. Additional blocks may be required to promote the correct orientation when the chain leaves the surface (Joint, J, segments) and to allow identification (segment I) of the polymer during either purification or characterization (*e.g.* epitope for immunodetection or aromatic groups for identification by UV spectrophotometry if such groups are not present in the other blocks). This architecture could, for example, be used to tether an active enzyme, or a receptor above a surface (active block = enzyme).

In this study, this unnatural protein design has been applied for the control of surface forces between alumina particles. Hence, our active element is a hydrophilic block designed so that restriction of this element to a smaller volume requires an input of energy, and therefore produces a repulsive, stabilizing force. Thus, the same group can perform the task of spacer and active element. In addition, we have not yet incorporated specific joint or identification segments. We have synthesized a polypeptide-based

polymer in which the active element consists of two blocks, a homopolymer of L-proline, Pro_{39}, and a recombinant form of the natural protein thioredoxin.

A poly-L-proline block was chosen because it is water soluble. Proline is an unusual amino acid because it is the only one of the twenty common amino acids that is cyclic. The five-membered ring that spans the α-carbon and the nitrogen leads to a restriction of rotation about the α-carbon–carbonyl bond and therefore the existence of *cis* and *trans* forms of the monomer at room temperature. The existence of a significant fraction of *trans* conformations leads to a larger persistence length than for other neutral homopeptides. The unnatural protein that we describe in this paper includes a block of 39 proline monomers. Using the wormlike chain model,[33] we calculate the root-mean squared end-to-end distance of the Pro_{39} block, $R_{RMS} \sim 7.1$ nm. (**$C_\infty = 13.7$** in water;[34] effective bond length, $l_0 = 0.38$ nm; the number of segments, $n = 39$). So an isolated Pro_{39} is expected to have a distance of about 7 nm between its N- and C- termini in water and a radius of gyration, R_g, of approximately 2.8 nm. There is still some disagreement over the length of polyproline oligimers in solution so the above figures should be treated as approximate. We have not used a Gaussian chain model because there are only about three statistical segments. The structure is known to depend on the solvent conditions, and in particular, is known to adopt a shorter conformation in concentrated salt solutions.[34] Earlier work showed that polyproline adsorbs only very weakly to the surface of alumina, so the polyproline block should not lie flat on the surface.[35]

An engineered version of thioredoxin, HP-Thioredoxin (Trx), was included as a fusion protein to aid in the expression, detection and purification of the unnatural protein. Trx is a mutant in which the glutamic acid (Glu) residue at position 32 and the glutamine (Gln) residue at position 64 have been replaced with histidine residues.[36] When the protein folds into its native 3-dimensional structure, these histidines, along with a native histidine at position 8, form a 'histidine patch' on the protein surface. Histidine patches have been shown to have high affinity for divalent cations and, therefore, can be used to easily purify the fusion protein on metal chelating resins.[37] Trx also improves the solubility of the recombinant protein products.[37]

The key feature of Trx is that of the 113 amino acids in the protein, 13 are acidic and 14 are basic (including 3 partially charged histidine residues), so at neutral pH the

protein has a low *net* charge density (the isoelectric point is pH = 6.3). Thus, the force contribution from adsorbed Trx layers should be relatively insensitive to salt and pH in the neutral range. The acidic and basic monomers are spread roughly evenly through the primary sequence and in the folded structure.[38] The approximate size of the thioredoxin in the crystal structure is 2.5 nm × 3.4 nm × 3.5 nm.[39]

In this paper, we demonstrate the use of the unnatural protein, Trx-$Pro_{39}Glu_{10}$, to the control of surface forces acting on an alumina particle. Alumina has a large Hamaker constant in water, and is therefore unstable in concentrated salt solutions. Because alumina is positively charged at neutral pH, it can be dispersed in water through the adsorption of anionic polymers[19,40,41,42,43,44,45] or through the adsorption of diblock copolymers. [19,26,46] We have used two approaches to find the anchor block: rational design, and a combinatorial search. For the rational design, we used the obvious path of imitating our predecessors with a polyacid, a decamer of glutamic acid (Glu_{10}). Our earlier work showed that poly(glutamic acid) adsorbs to alumina from dilute solutions, and that poly (glutamic acid) adsorbs almost exclusively from mixtures of poly(glutamic acid) and polyproline.[35]

To summarize, Figure 4.4 shows a schematic of our target polypeptide and our target adsorbed polymer layer. We expected that the Glu_{10} block would adsorb strongly to the alumina and also approximately neutralize the surface. We expected that the Pro_{39} block would not adsorb to the alumina, and that the Trx domain would be situated well away from the surface owing to the solubility of the Pro_{39} block. Trx is approximately neutral, so the net electrostatic forces between polymer coated surfaces should be small. The existence of a water-rich region between the Trx and the alumina surface should greatly reduce the van der Waals force between the adsorbed layers in water. In practice, our results show that the surface forces between alumina bearing adsorbed layers of protein do exhibit a long-range repulsion that is independent of salt concentration, as required for colloidal stability.

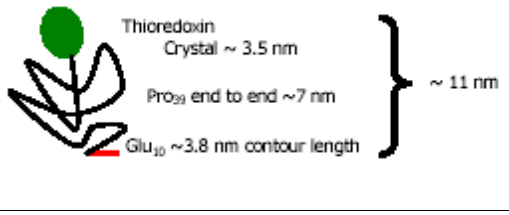

Figure 4.4 Schematic representation of Trx-$Pro_{39}Glu_{10}$ structure and hypothetical structure of adsorbed polymer layer.

4.2.3 Results and Discussion

Protein Purification and Identification. The Trx-$Pro_{39}Glu_{10}$ was expressed at a level of 40 mg product/L and purified by a sequence of IMAC, ion exchange, and gel filtration chromatography. The Trx-$Pro_{39}Glu_{10}$ product adsorbed strongly to the IMAC column resin and was eluted with a pH 4 buffer. As shown in the SDS-PAGE gel of Figure 4.5, the Trx-$Pro_{39}Glu_{10}$ product (Lane 4) migrates at an apparent molecular weight of 26 kDa, which is higher than its calculated molecular weight based on amino acid sequence of 17.3 kDa. The size discrepancy between expected and measured Trx-$Pro_{39}Glu_{10}$ product molecular weight is likely due to aberrant SDS binding to the $Pro_{39}Glu_{10}$ portion of the product. During SDS-PAGE, SDS binds to most proteins with a ratio of 1 dodecyl sulfate molecule per 2 amino acid residues.[47] Bound SDS causes denaturation of the protein and gives most proteins the same charge-to-mass ratio.[48] Hence, the negatively charged protein-SDS complexes migrate through the polyacrylamide gel towards the positive cathode and are separated only by their size. We hypothesize that the $Pro_{39}Glu_{10}$ portion of the product does not bind SDS as effectively as 'normal' globular proteins, causing it to migrate more slowly through the gel, as if it were a larger molecule.

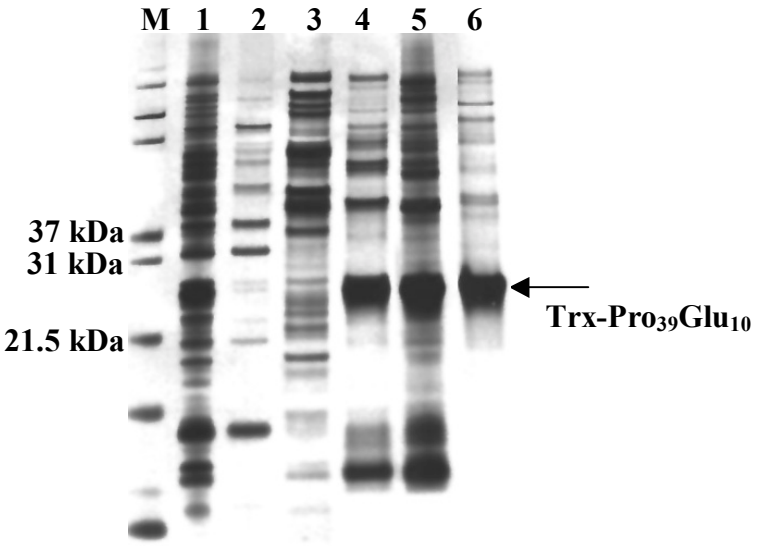

Figure 4.5 Silver stained SDS-PAGE showing purification of Trx-$Pro_{39}Glu_{10}$. Lane 1, IMAC feed; Lane 2, IMAC flow-through; Lane 3, IMAC pH6 Wash; Lane 4, IMAC pH4 Elution; Lane 5, IEC feed; Lane 6, IEC eluate. The Trx-$Pro_{39}Glu_{10}$ product is indicated by arrow.

The Trx-$Pro_{39}Glu_{10}$ product was further purified by anion exchange chromatography, exploiting the strongly negative charge of Glu_{10} block (Figure 4.5, Lane 6). After polishing by gel filtration, the purity of the Trx-$Pro_{39}Glu_{10}$ was determined by densitometry of Coomassie Blue-stained SDS-PAGE gels. As shown in Figure 4.6, it was determined that the polished Trx- $Pro_{39}Glu_{10}$ product was >98% pure.

The Trx-$Pro_{39}Glu_{10}$ identity was confirmed by amino acid analysis. The expected 44 moles proline/mole protein was detected, along with the expected amounts of Glx (Glu + Gln), His, and other amino acids. In summary, from the DNA sequence results and the amino acid compositional analysis, we confirmed the identity of the highly purified product to be the HP-Thioredoxin protein containing a C-terminal $Pro_{39}Glu_{10}$ polypeptide.

A HP-Thioredoxin protein was also expressed from the pThioHisA vector (Invitrogen) to serve as a control for the adsorption experiments. The control Trx was expressed and purified in the same manner as the Trx-$Pro_{39}Glu_{10}$ product. The identity of the control Trx was confirmed by DNA sequencing and cross-reactivity with the Anti-Thio™ antibody (data not shown). As shown in Figure 4.6, the polished control Trx product was >98% pure. As a result of using the pThioHisA vector, the C-terminus of

this control Trx contained an extra 30 amino acids (GDDDDKVPWEPEIFEFRGRRPLESTCSNRTG) resulting from the multiple cloning site of the vector that were not present in the Trx domain of Trx-$Pro_{39}Glu_{10}$. This stretch of extra amino acids on the C-terminus of the control Trx confers a slightly negative charge at pH~7 due to the excess of acidic monomers (7) over basic monomers (5). Thus, one might expect slightly greater adsorption of the Trx control than for a control that exactly matched the Trx domain of our fusion polymer.

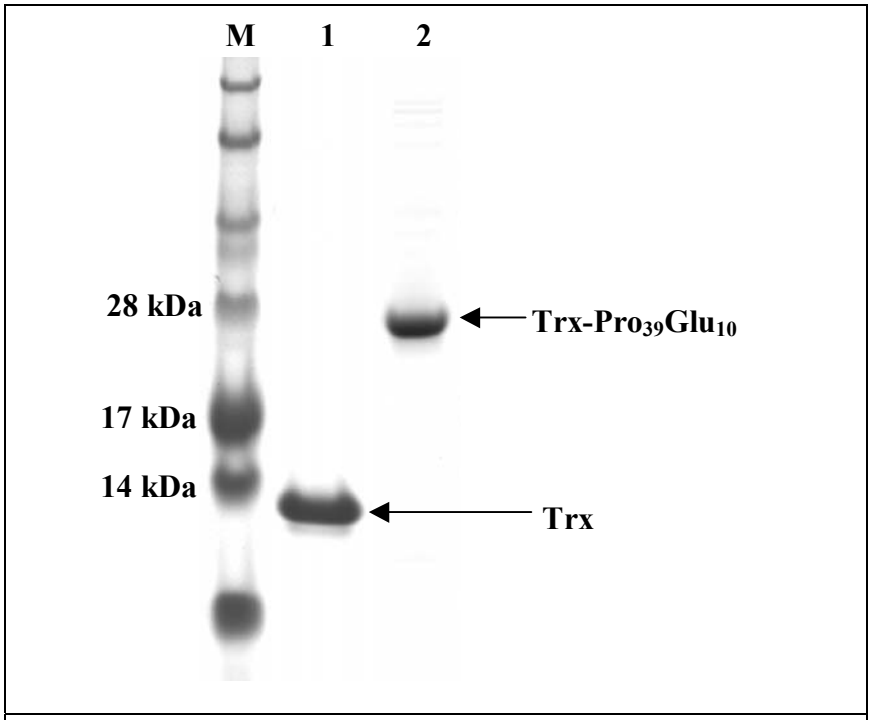

Figure 4.6 SDS-PAGE gel used for purity analysis of the products using densitometry. Lane 1, polished control Trx product (>98% pure); Lane 2, polished Trx-$Pro_{39}Glu_{10}$ product (>98% pure).

Solution Light Scattering. Dynamic light scattering of Trx-$Pro_{39}Glu_{10}$ solutions at pH ~ 7 in deionized water at 25°C showed two peaks: a peak with mean hydrodynamic radius R_H ~ 5 nm that accounts for approximately 90% of the sample by mass and a peak with mean hydrodynamic radius ~30 nm that accounts for approximately 10% of the sample by mass. The 5 nm fraction is consistent with a single chain with the primary sequence of the fusion protein. The ~30 nm fraction is consistent with the presence of aggregated molecules.

Characterization of the Alumina Surfaces. Figure 4.7 shows the forces between an oxygen plasma treated polycrystalline alumina particle of radius, R, and a single crystal sapphire plate as a function of pH in 1 mM KNO_3 solution. The forces, F, are normalized by R because $F/2\pi R$ is equal to the energy of interaction per unit area of one flat surface interacting with an infinite plate plate, E_a, when the surfaces are homogeneous and the range of the force is much less than R.[49]

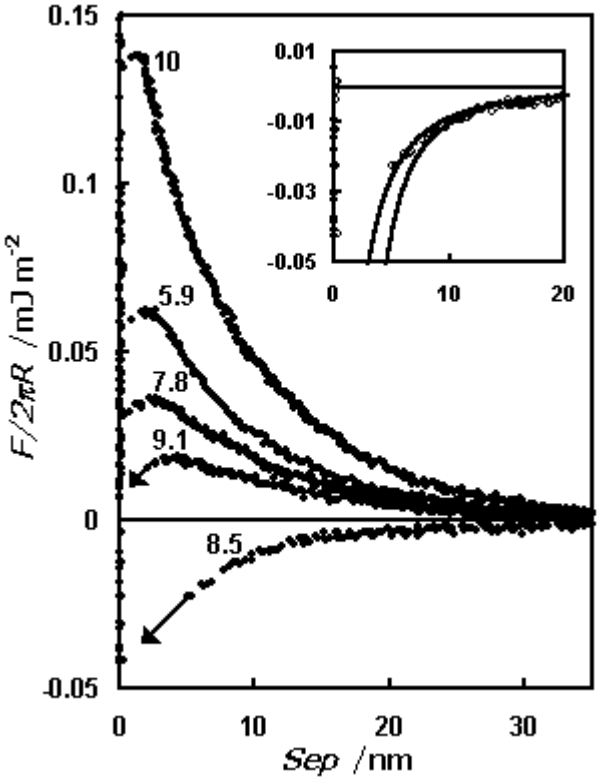

Figure 4.7 Forces between an alumina sphere and a sapphire plate in 1 mM KNO_3 solution. The force as a function of pH passes through a minimum at pH 8.5. The inset shows the pH 8.5 data together with the fitted van der Waals force. The best fits are obtained for $A = 4\times10^{-20}$ J (right curve) or $A = 5\times10^{-20}$ J with the zero of the van der Waals force shifted by 2.1 nm (left curve). Surface potentials obtained from fits to DLVO theory and forces required to separate the surfaces from contact (adhesive force) are as follows: pH 5.9: $\psi = 26$ mV, F/R = 0; pH 8: $\psi = 24$ mV, F/R = 0 mNm^{-1}; pH 8.5: $\psi = 0$ mV, F/R= –0.2mNm^{-1}; pH 9: ψ = –20 mV, F/R = –0.07 mNm^{-1}; pH 10: ψ = , –36 mV F/R = 0.005 mNm^{-1}. The surface potentials were calculated from DLVO theory with a Hamaker constant of 5×10^{-20} J. The magnitude of each potential is increased by about 2 mV if the van der Waals force is shifted by 2.5 nm. The change in sign of the potentials is inferred from the minimum in force.

There is a minimum in the force at about pH 8.5, indicating the loss of double-layer forces and therefore a point of zero charge (pzc) at about 8.5. If we fit this force to a van der Waals force, using the onset of constant compliance as zero separation, then we obtain a non-retarded Hamaker constant of 4×10^{-20}J. This is smaller than predicted theoretically by Hough and White (5.3×10^{-20}J)[7] and measured previously by Horn *et al*. (6.7×10^{-20}J),[50] which is consistent with the observation that the particle is rough (~ 3 nm over 1 μm^2). At zero separation in our figures, the particle is probably resting on asperities, not in smooth contact. If we shift the zero of the theoretical van der Waals force to –2.1 nm, then the fitted Hamaker constant is about 5×10^{-20}J.

Horn *et al*. found a pzc of about 6.7 through their force measurements.[50] In separate experiments, when we measured the forces without an oxygen-plasma treatment of the surface, we found that the pzc was about 5–6. For all other experiments reported here, we plasma-treated the surfaces so as to obtain a pzc of 8–9, so that our results could be applied to particulate alumina of the same pzc. Clearly the pzc of our alumina depends on the surface treatment; for a review of the differences in pzc between crystalline and particulate alumina, the reader is referred to the work of Franks and Meager.[51] For some particles, a pzc of 8–9 could not be obtained, so these particles were discarded.

The force increases when the pH deviates to higher or lower pH than the pzc of 8.5. The surface potentials are similar to those measured previously by Horn *et al*. After making measurements in pH 10 solution, the forces at pH 6 were altered: the pzc was lower. So all measurements in Trx-$Pro_{39}Glu_{10}$ solution were performed on surfaces that were never exposed to solutions of pH > 8.5.

Adsorption and Forces in the Presence of Trx-$Pro_{39}Glu_{10}$. The density of Trx $Pro_{39}Glu_{10}$ adsorbed to the sapphire plate from a 0.1 mg/mL solution in 1 mM KNO_3 was determined by ellipsometry. The lack of optical contrast between sapphire, the polymer, and water forced us to adsorb the protein from solution, and then to measure the adsorption after rinsing in salt solution, then water, then drying of the plate with N_2 gas. Force measurements were made after the same rinsing procedure (see below). The density of adsorption was 4–10 nm^2/molecule (2.8–7.2 mg/m^2). The large error arises because of the lack of optical contrast of the thin film. The approximate cross-section of

the thioredoxin crystal structure is 8–12 nm^2.[38] As the range of measured adsorption areas has a maximum that is roughly equal to the cross-sectional area of a thioredoxin molecule in the crystalline state, it appears that the physical dimensions of Trx may limit adsorption. In fact, the range of measured areas includes values smaller than the crystal dimensions so it is possible that some of the Trx segments might be adsorbed directly onto the alumina surface as shown in Figure 4.4. R_g for a free Pro_{39} chain in aqueous solution is approximately 3 nm (from the wormlike chain calculation), so the Pro_{39} block has been confined to a smaller cross-sectional area on the surface than a free Pro_{39} block in solution. This lateral confinement should also lead the adsorbed Pro_{39} block to have a greater extension normal to the surface than when free in solution.

Surface forces with adsorbed Trx-$Pro_{39}Glu_{10}$ layers were measured by the following procedure. First, we measured the force in KNO_3 solution as a function of pH. We only continued if the pzc was ~ 8.5. The surfaces were then exposed to a 0.1 mg/mL aqueous solution of Trx-$Pro_{39}Glu_{10}$ in 1 mM KNO_3 for about 12 hours. The forces were measured in the presence of Trx-$Pro_{39}Glu_{10}$, and then again after rinsing with 1 mM KNO_3. The forces were usually slightly longer-ranged and more hysteretic in Trx-$Pro_{39}Glu_{10}$ solution than in KNO_3, suggesting that there was some weakly and reversibly adsorbed Trx-$Pro_{39}Glu_{10}$ that was easily removed by rinsing. All forces shown here were measured after rinsing.

Figure 4.8 shows the forces between alumina surfaces bearing adsorbed Trx-$Pro_{39}Glu_{10}$ at pH ~6 (unbuffered). After adsorption of a polymer, it is not possible in general to determine the separation compared to the contact between the alumina surfaces in AFM force measurements. The zero of our distance scale represents the separation at which the sphere encounters a steep repulsive wall: there the polymer film is less compliant than the spring. However, the polymer film still has a finite thickness at this position, so we have indicated our uncertainty with the shaded area between 0 and –10 nm.

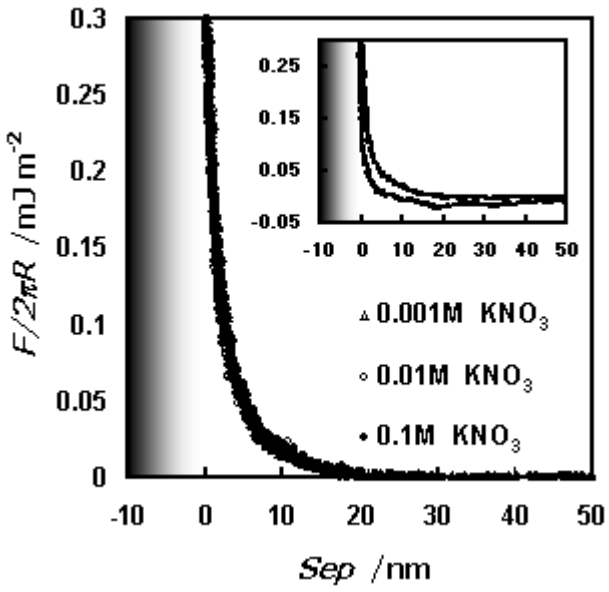

Figure 4.8 Forces on approach between an alumina sphere and a sapphire plate in KNO_3 solutions at pH ~ 6 after the surfaces have been exposed to a 0.1 mgmL^{-1} Trx- $Pro_{39}Glu_{10}$ solution in 1 mM KNO_3, and then rinsed with 1 mM KNO_3 solution. Trx- $Pro_{39}Glu_{10}$ remains adsorbed to the alumina solid, and the force is independent of the salt concentration. The inset shows the typical hysteresis between the force on approach (upper) and separation (lower). The shaded region between 0 and –10 nm is a reminder that we do not know the absolute separation between the Al_2O_3 surfaces.

Figure 4.8 shows that the force is now approximately independent of the salt concentration at all separations and thus double-layer forces are negligible. We have created the desired repulsive force for colloidal processing that is repulsive and is independent of salt concentration. The proposed mechanism is that the Glu_{10} block has neutralized the alumina charge and the Trx-Pro_{39} blocks are providing steric stabilization by forming a brush-like layer at the surface. We know that the Glu_{10} segment has enough capacity to neutralize the alumina charge because the ellipsometry measurements show that the protein density is 0.1–0.25 molecules/nm^2, and therefore the capacity to neutralize the alumina charge is 1–2.5 e/nm^2. In comparison, the surface forces measurements in the absence of protein are consistent with an alumina surface charge of 0.012 e/nm^2. Both the alumina and the carboxylic acid can regulate their charge density by proton adsorption/desorption so the charged state of each is not known when the protein is adsorbed. Thus, it is possible that the surface could become charged at other pH values.

In Figure 4.9, the forces are plotted on a semi-log scale to show that the force is exponential with a decay length of 5.2 ± 0.5 nm. If we were to model the adsorbed layer as a brush, Equation 1 suggests that the brush length should be ~15–18 nm. This is longer than expected from the dimensions of the proline (~7 nm) and thioredoxin (~3.5 nm) blocks and so would require extension of the molecule. However, Equation 1 is based on a brush structure and we do not have a classical brush.

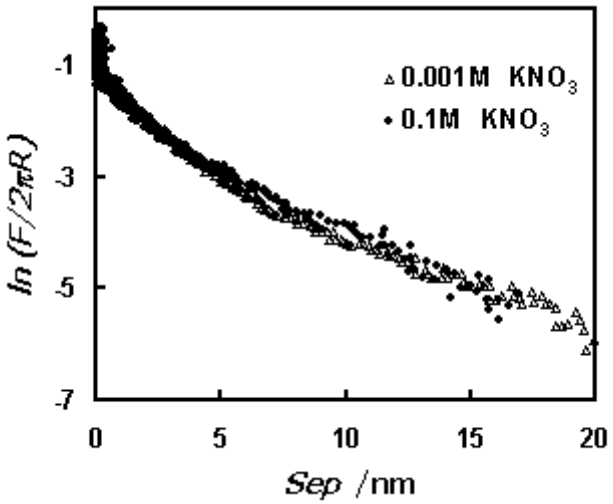

Figure 4.9 Natural log of data from Figure 4.8 showing that force decay is approximately exponential. The decay length is 5.2±0.5 nm.

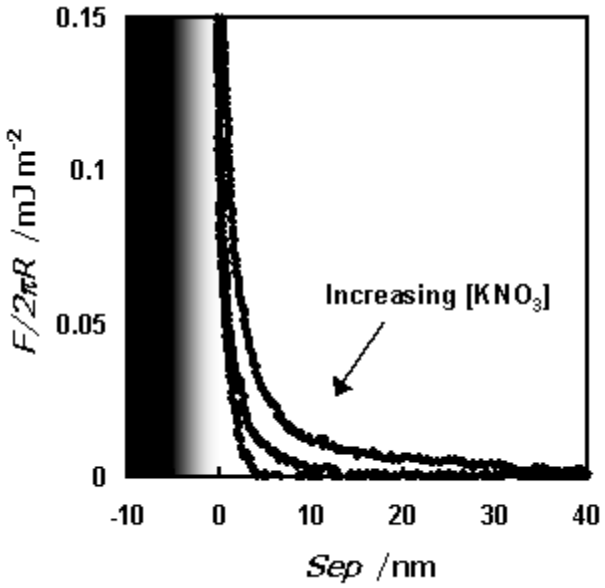

Figure 4.10 Forces on approach between an alumina sphere and a sapphire plate in KNO_3 solutions at pH ~ 6 after the surfaces have been exposed to a 0.1 mgmL^{-1} Trx solution in 1 mM KNO_3 then rinsed with 1 mM KNO_3 solution. The protein remains adsorbed to the alumina solid after rinsing. Forces are shown in three salt concentrations, 0.001 M (most repulsive), 0.01 M, 0.1 M (least repulsive).

In contrast, Figure 4.10 shows the force in the presence of adsorbed Trx that that does not have the $Pro_{39}Glu_{10}$ tether. The force is repulsive, but the force decreases with salt concentration. The reduction in the range with increased salt concentration shows that there is a double-layer or electrosteric force between the surfaces. Since the Trx is approximately neutral, this result suggests that the adsorption has not neutralized the alumina charge. So the role of the anchor block in our Trx-$Pro_{39}Glu_{10}$ fusion protein is not only to anchor the protein to enable steric forces, but also to neutralize the alumina charge. Support for the hypothesis of electrostatic forces comes from the correlation between the decay length of the force and the theoretical Debye-length, as shown in Table 4.1.

$[HNO_3]$ mol L^{-1}	Decay Length nm	κ^{-1} nm
0.001	9.9 ± 2.6	9.5
0.01	3.4 ± 0.7	3.0
0.1	1.5 ± 0.5	0.95

Table 4.1 Comparison between the decay length of measured forces between Trx-coated alumina and the theoretical Debye-length.

Recall that our Trx control is not identical to the Trx domain in Trx-$Pro_{39}Glu_{10}$: the control protein has an additional 30 amino acids, 5 positive and 7 negative, which make the protein slightly negative at neutral pH. If these additional monomers have an effect, it is likely to enhance adsorption and neutralization of the positively-charged alumina, but clearly the effect is not enough to produce the desired forces.

Combinatorial Search for an Anchor Block. Finally, we attempted to discover an optimal block to anchor the polypeptide to alumina through a combinatorial search using a (bacterial) FliTrx™ library in PBS buffer.[42] The buffer was included to aid the growth and survival of the bacteria. The bacteria in the library display one of a library of proteins on their surface, which modulate adhesion to a surface. The alumina plate was exposed to a solution containing a bacterial library and bacteria were allowed to adsorb to the surface. The plate was then withdrawn from solution, thereby selecting for bacteria bearing proteins that have binding sequences. After emersion, the adhering bacteria were amplified and the alumina was exposed in repeated cycles to the previously adhering bacteria until the strongest adhering sequences were found.

The sequences that we found were all cationic, which was at first surprising. However, zeta potential measurements showed that the potential on alumina particles changed from positive to negative in the presence of the phosphate buffer, presumably through adsorption of divalent phosphate. This highlighted, for us, the necessity of performing the combinatorial search under the same conditions as for the application of the polymer. In future work, it would be better to use a library that can survive under conditions that are more similar to those under which the adsorption will be implemented (*e.g.* a bacteriophage display library[32]).

4.2.4 Conclusions

We designed and synthesized, using recombinant DNA techniques, a polypeptide to act as a steric stabilizer on a charged metal oxide surface in water. The protein consisted of an anionic (Glu) anchor block, an uncharged (Pro) block, and a Trx domain that, under the experimental conditions was essentially uncharged. Ellipsometry measurements showed that this copolypeptide adsorbed from an aqueous solution at pH ~ 6–7 onto a positively charged alumina surface. AFM measurements showed that adsorption generated a steric force and made the double-layer force insignificant. The forces in the presence of adsorbed polymer are suitable for colloidal processing. Synthesis via recombinant DNA techniques can produce a very wide variety of polymer sequences, so the methods described here could be applied to adsorption to other solids, and to a wide variety of stabilizing elements. A further advantage of synthesis via recombinant DNA techniques is that there is a ready palette of natural functional proteins that can be incorporated into polymer designs.

4.2.5 Acknowledgements

The authors acknowledge the help of the late Dr. Christopher G. Russell, formerly of Invitrogen, who consulted and aided in the cloning of the initial Trx-ProGlu genes. This work is based on research supported by the National Science Foundation Grant BES-0086876 and the Petroleum Research Fund under Grant number 36327-AC5. The authors acknowledge assistance by Dr. Felicia Etzkorn, Dr. Luke Mosley, Myles Lindsay, Weslyn Ward and Nurxat Nueraji.

4.2.6 Materials and Methods

Materials for Protein Expression. HS996 and One Shot® TOP10F' Chemically Competent *E. coli* strains, His-Patch ThioFusion™ Expression System, NuPAGE® Novex 10% Bis-Tris polyacrylamide gels, Anti-Thio™ antibody, LB Broth Base, UltraPure™ agarose, UltraPure™ ethidium bromide solution, Mark12™ Unstained Protein Standard, SeeBlue® Plus2 Pre-Stained Protein Standard, synthetic oligonucleotides and DNA primers were purchased from Invitrogen Corp. (Carlsbad, CA). *Taq* PCR Core Kit, QIAprep® Spin Miniprep and QIAquick® Gel Extraction/PCR Purification Kits were purchased from Qiagen, Inc. (Valencia, CA). LB Agar, CelLytic™ B Bacterial Cell Lysis Extraction Reagent, Coomassie Brilliant Blue R250, and glycerol were obtained from Sigma (St. Louis, MO). Ampicillin, isopropyl β-*D*-thiogalactopyranoside (IPTG) and 0.2 μm pre-sterilized syringe filters were purchased from VWR International (So. Plainfield, NJ). Immun-Blot® PVDF membrane was purchased from Bio-Rad Laboratories (Hercules, CA). Chelating Sepharose Fast Flow, DEAE Sepharose Fast Flow, and Sephadex G-25C were obtained from Amersham Biosciences (Piscataway, NJ) for chromatography applications. SnakeSkin® Pleated Dialysis Tubing (3 kDa molecular weight cutoff) was purchased from Pierce (Rockford, IL). All restriction enzymes, DNA modifying enzymes, T4 DNA Ligase, 100 bp DNA and 1 kbp DNA Ladders were all purchased from New England Biolabs (Beverly, MA).

General Methods for Biosynthesis. The procedures for the manipulation of DNA, transformation, cell growth, product expression and analysis were adapted from published literature[52,53] or from instructions provided by product manufacturers. All reagents for the manipulation of DNA were sterile and DNAse/RNAse free. Enzymatic manipulations of DNA were conducted in reagent buffers supplied by the manufacturer. PCR amplification and DNA extension reactions were performed in an Omnigene thermal cycler from Hybaid (United Kingdom). Automated DNA sequence analysis was performed on a Perkin-Elmer ABI Prism model 377 DNA Sequencer at Cleveland Genomics, Inc. (Cleveland, OH). Cells were lysed using a Tekmar Sonic Disruptor with a microtip sonicator (Mason, OH). Product analysis was conducted by SDS-PAGE using pre-cast NuPAGE Novex 10% Bis-Tris polyacrylamide gels on an Xcell Surelock Mini-Cell apparatus from Invitrogen Corp. The gels were visualized using a silver staining protocol adapted from published literature[54] or by Coomassie Blue staining. Polyacrylamide gel images were captured using a Microtek ScanMaker X6EL scanner. Polypeptide product and DNA concentrations were calculated from the optical density (OD) obtained using a Milton Roy Spectronic 1201 UV spectrophotometer (Ivyland, PA). All chromatographic separations were conducted on a Bio-Rad BioLogic DuoFlow system with 280 nm and 214 nm detection.

Construction of Pro_mGlu_n Gene (Figure 4.11). Two single-stranded oligonucleotides of 107 bases each with complimentary 3' ends and an ultimate coding capacity of $Pro_{40}Glu_{10}$ were purchased. To construct the gene, the sense and antisense oligonucleotides were mixed and then heated to 95°C. The mixture was cooled down slowly to 5°C below the estimated melting temperature (T_m) of the oligonucleotides and held for 5 minutes to anneal the complimentary bases. A solution of dNTPs was added, followed by the addition of *Taq* DNA Polymerase to begin the 'fill-in' reaction. Agarose electrophoresis showed that the average product size was ~180 base-pairs, as desired (data not shown). A *Mlu*NI site was incorporated into the 5' end of the synthetic gene, just upstream of the proline codons and an *Xba*I site at the 3' end, downstream of the glutamate codons. The product was then digested with *Mlu*NI and *Xba*I. The *Mlu*NI digest resulted in a blunt end at the 5' end. The *Xba*I digest allowed for convenient insertion into the vector, pThioHisA. This vector was sequentially digested with *Asp*718I and Mung Bean Nuclease to form a blunt end, followed by digestion with *Xba*I. The Pro_mGlu_n gene was ligated into the linearized vector with T4 DNA Ligase and transformed into HS996 *E. coli* (Figure 4.11A). Transformants were selected on LB agar containing 100 μg/ml ampicillin. Thirty colonies were picked and plasmids were isolated from each using a standard alkaline lysis protocol.[52] The recombinant plasmids were digested with *Sma*I and *Xba*I to identify clones with inserts of the correct size. Plasmids from 2 positive clones were purified and were submitted for DNA sequence analysis. Stocks of these clones were made in 15% glycerol and stored at -80°C.

The Pro_mGlu_n gene was then PCR subcloned (Figure 4.11B) to include an Asn-Gly-Gly tripeptide between the C-terminus of the Trx and the N-terminus of the Pro_mGlu_n polypeptide. This tripeptide sequence was designed to provide the additional option in the future to remove the Trx fusion tag by chemical cleavage with hydroxylamine, which cleaves the peptide bond between Asn-Gly.[55,56] The Pro_m-

Glu_n gene was PCR amplified from the recombinant vector using the following primer set: [Forward: 5'-attaggatccaacggtggtcctccccctcctcctcct-3'; Reverse: 5'-gtcgactctagagctattcttcttc-3']. The amplifying primers also contained restriction enzymes sites for *Bam*HI and *Sal*I for convenient cloning into the expression vector, pThioHisA. Using *Taq* DNA polymerase and an annealing temperature of 62°C, a new double-stranded Pro_mGlu_n gene was amplified. After purification, the PCR product and expression vector were digested with *Bam*HI and *Sal*I overnight (~16 hours) at 37°C and ligated in a 3:1 insert:vector molar ratio with T4 DNA Ligase overnight (~16 hours) at 16°C. The ligation reaction was transformed into One Shot® TOP10F' Chemically Competent *E. coli* and selected on LB agar plates containing 100 μg/ml ampicillin. Colonies were selected and used to inoculate 5 ml of LB Broth containing 100 μg/ml ampicillin and incubated for 16 hours at 37°C. Plasmids were isolated using the QIAprep® Spin Miniprep kit. Plasmids from several colonies were submitted for DNA sequencing to Cleveland Genomics, Inc. using Trx sequencing primers (Invitrogen) to validate gene sequence and orientation. The analysis yielded the following sequence downstream of the Trx gene: 5'- aac ggt ggt cct ccc cct cct cct cct cct ccc cct cct cct cct cct cct cct cct cct cca cct ccg ccg cca ccc ccg cct cca cca cca cca cca cca cca cca cca cca cca gaa gaa gaa gaa gaa gaa gaa gaa gaa gaa gaa tag -3'. This DNA sequence agreed with the target sequence and encodes for the amino acid sequence H_3^+N-Asn-$Gly_2Pro_{39}Glu_{10}$-COO^- which is fused to the C-terminus of the Trx fusion protein. Stocks were made of the positive clone by adding glycerol to a final volume of 15% and these were stored at -80°C.

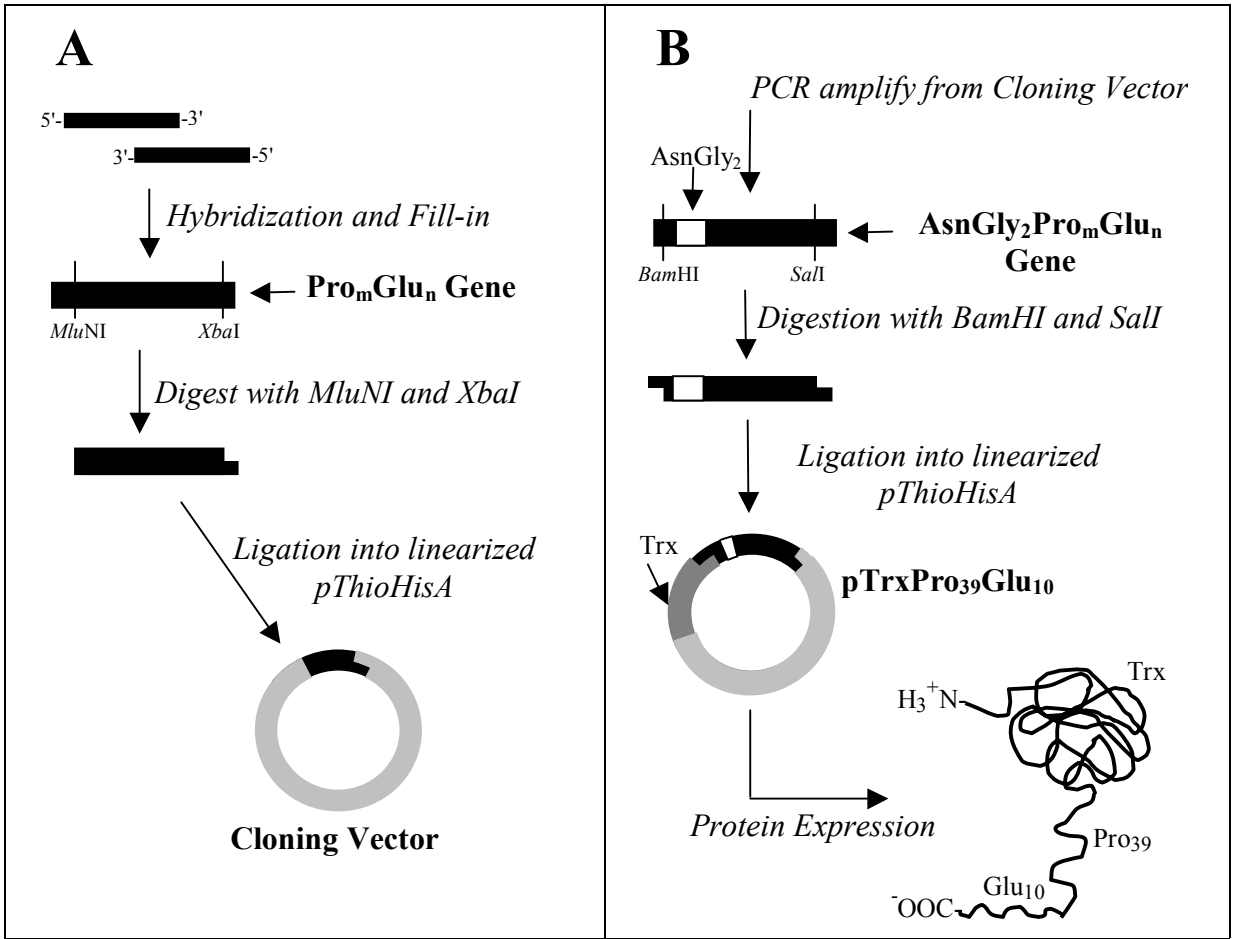

Figure 4.11 Schematic showing the construction of the Pro_mGlu_n gene (Panel A) and the PCR subcloning of the Pro_mGlu_n gene into the expression vector, forming $pTrxPro_{39}Glu_{10}$ (Panel B).

Product Expression. In a 250 mL culture flask, 50 mL of LB Broth containing 100 µg/mL ampicillin was inoculated with stock bacterial culture containing the recombinant vector pTrxPro$_{39}$Glu$_{10}$. The culture was incubated overnight at 37°C with shaking at 200 rpm. The culture was pelleted in a 50 mL centrifuge tube at 3000 X ***g*** for 10 minutes at 4°C. The supernatant was removed and the pellet was re-suspended in 10 mL of fresh LB media. Four 1 L culture flasks with 250 mL of fresh LB media containing 100 µg/ml ampicillin were inoculated with 2 mL of this cell suspension. The culture was incubated at 37°C with shaking at 200 rpm until mid-log phase (OD_{600} ~ 0.5). Expression of Trx-Pro$_{39}$Glu$_{10}$ product was induced by the addition of IPTG to a final concentration of 1mM, and the cultures were incubated for an additional 5-6 hours. The cells were harvested by centrifuging at 3000 X *g* for 10 minutes at 4°C, and the pellets were stored at -80°C. This procedure was repeated for the expression of Trx from a TOP10 strain containing the pThioHisA control expression vector that is available with the pThioHis expression kit from Invitrogen.

Cell Lysis. Approximately 1 mg of wet cell pellet was re-suspended in 15 mL of CelLytic™ B Bacterial Cell Lysis Extraction Reagent. The cell suspension was sonicated with a Tekmar Sonic Disruptor with a microtip sonicator (Mason, OH) with four 10 second bursts while keeping the samples on ice. The samples were then frozen at -80°C followed by a rapid thaw in a 42°C water bath. This sonication/freeze/thaw procedure was repeated 4 times. After the final round, an appropriate volume of 5X IMAC Binding Buffer was added to make a 1X solution (20 mM sodium phosphate, 0.5 M NaCl, pH 7.8). Cell debris was centrifuged at 13,000 X *g* for 15 minutes at 4°C. The soluble cell extract containing the Trx-Pro$_{39}$Glu$_{10}$ was collected and cell debris pellet was discarded.

Immobilized Metal Affinity Chromatography Purification. Purification of the Trx- Pro$_{39}$Glu$_{10}$ product from the soluble cell extract was accomplished by immobilized metal affinity chromatography (IMAC) using a column packed with Chelating Sepharose Fast Flow (8 cm x 2.5 cm i.d.) charged with Ni^{2+} (100 mM $NiCl_2$) and equilibrated in 1X Binding Buffer. Cell extract in 1X Binding Buffer was loaded onto the column at a flow rate of 0.8 cm/minute. The column effluent was monitored at 214 nm. The column was washed with 2 column volumes (CV) of 1X Binding Buffer. Weakly bound proteins were eluted with 4 CV of 20 mM sodium phosphate, 0.5 M NaCl pH 6. The Trx-Pro$_{39}$Glu$_{10}$ product was eluted with 4 CV of 20 mM sodium phosphate, 0.5 M NaCl pH 4. The pH of the eluate sample was adjusted to pH~7 with 4 M NaOH. Following elution, the column resin was re-equilibrated with 4 CV of Binding Buffer. All steps were conducted at a linear flow rate of 0.8 cm/min. The fractions containing the Trx- Pro$_{39}$Glu$_{10}$ product were pooled together. Product concentration was estimated by measuring the OD at 280 nm (assuming an extinction coefficient of 0.834 L/(g·cm) calculated based on the amino acid sequence of the product[57]). Samples were stored at -80°C. This procedure was also repeated for the purification of Trx (no fusion) from the control expression vector. The Trx-Pro$_{39}$Glu$_{10}$ products were dialyzed against deionized water using Snakeskin® Pleated Dialysis Tubing (3 kDa MWCO), lyophilized to dryness, and stored at -80°C.

Ion Exchange Chromatography Purification. Ion exchange chromatography (IEC) was used to separate the Trx-Pro$_{39}$Glu$_{10}$ product from other proteins that eluted from the IMAC column at pH 4. The dried sample was re-suspended in 1X IEC Loading Buffer: 20 mM Tris-HCl, pH 8.0 to a concentration of ~0.50 mg/mL. This solution was loaded onto a column packed with Diethylaminoethyl (DEAE) Sepharose Fast Flow (8 cm x 2.5 cm i.d.) that had been equilibrated with 1X IEC Loading Buffer. Following sample loading, the column was washed with 2 CV of 1X IEC Loading Buffer. Bound proteins were eluted with a linear gradient from 0-35% 20 mM TrisHCl, 1 M NaCl pH 8.0 over 10 CV at 0.5 cm/min. The column resin was regenerated with 3 CV of 20 mM sodium phosphate, 4 M NaCl pH 8.0, followed by re-equilibration with 1X IEC Loading Buffer. All steps with the exception of the salt gradient were conducted at a linear flow rate of 1.2 cm/min. The column effluent was monitored at 214 nm. The fractions containing the Trx-Pro$_{39}$Glu$_{10}$ product were pooled and concentration was measured by OD at 280 nm. The purified sample was then dialyzed and lyophilized as above.

Trx-Pro$_{39}$Glu$_{10}$ Polishing. Dried, purified Trx-Pro$_{39}$Glu$_{10}$ product was re-suspended in deionized water to a concentration of ~1 mg/mL. The solution was loaded (0.25 CV) onto a column packed with Sephadex G-25°C desalting resin. The column effluent was monitored at 214 nm. The fractions containing the desalted Trx-Pro$_{39}$Glu$_{10}$ product were pooled together and the concentration was measured by OD at 280 nm. The sample was frozen at -80°C and lyophilized to dryness. The product was then re-suspended in deionized

water to a concentration of ~5 mg/mL. Prior to surface adsorption studies, the purity and identity of the Trx-$Pro_{39}Glu_{10}$ product were confirmed by SDS-PAGE and amino acid analysis.

Purity Analysis. Product purity was determined using densitometry of SDS-PAGE gels. The purified sample was loaded onto an SDS-PAGE gel and stained with Coomassie Blue. The gel was then scanned using the Biorad GS-800 Imaging Densitometer. Using the accompanying software Quantity One®, the lane containing the product sample was analyzed for stained bands. The relative intensity of the bands were determined and compared to obtain the purity of the sample.

Trx-$Pro_{39}Glu_{10}$ Product Identity. The Trx-$Pro_{39}Glu_{10}$ product was characterized by amino acid composition analysis. Approximately 10 μg of the purified Trx-$Pro_{39}Glu_{10}$ was loaded onto 3 lanes of a SDS-PAGE gel. After electrophoretic separation, the sample was electroblotted onto PVDF membrane (BioRad) for 1.5 hours at 30 volts. After the transfer, the membrane was washed extensively with deionized water. The immobilized Trx-$Pro_{39}Glu_{10}$ product was stained with a 0.025% Coomassie Brilliant Blue R250 solution in 40% methanol for 5 minutes. The blot was de-stained in 50% methanol, followed by a deionized water wash. The blot was then dried and the bands corresponding to the Trx-$Pro_{39}Glu_{10}$ product were cut out. The bands were submitted to Commonwealth Biotechnologies, Inc. (Richmond, VA) for amino acid compositional analysis.

Materials for Adsorption Experiments. Water was purified with an EASYpure UV (Barnstead Thermolyne Corp., Dubuque, IA) that consisted of ion-exchange, charcoal, UV, and filtration stages. KNO_3 (Aldrich, Milwaukee, WI) was recrystallized twice from 200 proof ethanol (Aaper Alcohol Chemical Co., USA) and purified water (90:10). KOH (Aldrich, Milwaukee, WI) was roasted in air at 400ºC for 16 h. HNO_3 (Fischer Scientific, Fairlawn, NJ) was used as received. Single crystal alumina (sapphire) plates (Commercial Crystal Laboratories, Naples, FL) with a 12 mm × 12 mm (0001) surface (c-axis) had an rms roughness of <0.5 nm over 1 μm^2 and polycrystalline alumina spheres of radius ~ 15 μm (R.S.A. Le Rubis S.A., Jarrie, France) had an rms roughness of 3 nm over 1 μm^2. Prior to each experiment the sapphire plates were soaked in warm HNO_3 overnight and boiled in HNO_3 for one hour then allowed to cool and then rinsed with purified water. Both solids were treated with oxygen plasma (March Instruments, Concord, CA) for 3 min at 40 Watts at ~250 mTorr to render the surfaces hydrophilic and to remove organic material.

Solutions. Trx- $Pro_{39}Glu_{10}$ solutions were prepared in 1.5 ml Eppendorf tubes and electrolyte solutions were prepared in 30 mL. polycarbonate bottles (Nalge Company, Rochester, NY) to prevent contamination of the alumina surfaces by dissolved or colloidal silica. Polycarbonate bottles were soaked in 10 % Liqui-Nox solution (Alconox, White Plains, NY) overnight and rinsed with copious amounts of water, left in water overnight, rinsed with ethanol and again with water and left in water with caps on until use. They were rinsed with water prior to solution preparation. KOH and HNO_3 were used to adjust the pH of the solutions. Hydrogen ion activities were determined by a pH meter (Orion, Beverly, MA) and by a micro combination pH electrode (Lazar Research Laboratories, Los Angeles, CA) for protein solutions. Measurements were made relative to standard buffers of potassium hydrogen phthalate, pH 4.01 (Orion, Beverly, MA), pH 7.01 (Orion, Beverly, MA), and pH 10.01 (Orion, Beverly, MA).

Ellipsometry. A phase modulation ellipsometer[58] (Beaglehole Instruments, Wellington, New Zealand) with a HeNe laser (λ = 632.8 nm) was used to measure adsorption to a sapphire plate that was effectively a transparent dielectric, having only a small value of the imaginary component of the reflectivity, Im(r) ~0.005 at the Brewster angle, θ_B. Because the refractive index of the alumina plate is around 1.76,[59] the optical contrast between the alumina plate and water is too small for the accurate ellipsometric measurement and thus all measurements were performed in air after adsorbing Trx- $Pro_{39}Glu_{10}$ from aqueous solution. After adsorption of the polymer, the alumina plate was rinsed in exactly the same manner as for the AFM experiments, and then dried with nitrogen. The experiment was repeated four times and the results were consistent.

Changes in $I_m(r, \theta_B)$ due to an absorbed protein layer on the surface of alumina plate were calculated from the following equation:[60]

$$\mathrm{Im}(r,\theta_B)=\frac{\pi(\varepsilon_1+\varepsilon_2)^{1/2}(\varepsilon-\varepsilon_1)(\varepsilon-\varepsilon_2)}{\lambda(\varepsilon_1-\varepsilon_2)\qquad\varepsilon}z \tag{2}$$

For thin films, there is one measurable parameter, $\mathrm{Im}(r,\theta_B)$, but there are many combinations of the film dielectic constant, ε, and the film thickness, *z,* that satisfy Equation 2, so it is impossible to obtain the refractive index *n* and thickness *z* from one measurement. For this reason, the surface density reported in the Results has a large uncertainty. To limit this uncertainty, we have assumed that the thickness of the absorbed polymer layer in the *dried* state is less than 6 nm. Moreover, the refractive index of absorbed protein layers usually is larger than 1,[45,61,62] so we have set this as a lower

$$n = n_0 + c\frac{dn}{dc} \tag{3}$$

where n and n_0 are the refractive indexes of the absorbed protein layer and water respectively. The common values of the *dn/dc* of protein, in the range of 0.16–0.2 ml/g,[63,64,65] were employed in this study and it was assumed that *dn/dc* is the same in solution and in the (hydrated) film after removing the bulk water with nitrogen gas.

Atomic Force Microscopy (AFM). Force-Separation measurements were obtained with an AFM (Molecular Imaging, Phoenix, AZ). The cantilever holder in this device is made from fused silica so we always minimized contact of the AFM with basic solutions that could produce silicic acid. The alumina spheres were attached to AFM cantilevers as described previously[66] using 5-minute epoxy (Devcon, Riviera Beach, FL). The spring constants (~0.5 Nm^{-1}) of the tipless cantilevers (Ultrasharp noncontact silicon cantilevers NSC12, Silicon-MDT, Moscow, Russia) were determined by the Cleveland method.[67]

The z-axis of the piezo was calibrated by a silicon calibration reference of 22.0 nm step height (Silicon-MDT, Moscow, Russia). The calibration was cross-checked by measurement of decay length of double-layer forces in 10^{-3}, 10^{-2} and 10^{-1} $molL^{-1}$ KNO_3 solutions. Before the injection of the Trx-$Pro_{39}Glu_{10}$ solutions, the point of zero charge of sapphire was determined by obtaining force curves at different pH solutions at 10^{-3} M KNO_3. The electrolyte solutions were left inside the liquid cell for 15–30 min before data acquisition. The polymer solution was left inside the liquid cell for 12 hours during which time the surfaces were separated by 10μm and no force measurements were taken in order not to disturb the equilibrium adsorption of the protein. Multiple approach and separation runs were performed in each experiment and the entire experiment was performed three times (on different days). Measurements were performed in the temperature range 22 ± 2 ºC.

Light Scattering. The hydrodynamic radius R_H of Trx- $Pro_{39}Glu_{10}$ in pH~7 solution (1 mg/mL) at 25 ± 0.2 °C was measured by dynamic light scattering using a DynaPro-801TC (Proterion Inc. at a wavelength of 836 nm and at a fixed angle of 90°. Samples were filtered with a 1 μm PTFE (teflon) syringe filter. The radii were calculated with the Regularization algorithm.[68]

4.2.7 References

[1] Norrish, K. *Dis. Faraday Soc.* **1954**, *18*, 120-134.
[2] Ottewill, R. H. In *Concentrated Dispersions*; Goodwin, J. W., Ed.; Dorset Press: Dorset, 1982.
[3] Velamakanni, B. H.; Chang, J. C.; Lang, F. F.; Pearson, D. S. *Langmuir* **1990**, *6*, 1323-1325.
[4] Ducker, W. A.; Clarke, D. R. *Colloid Surface A* **1994**, *93*, 275-292.
[5] Ducker, W. A.; Luther, E. P.; Clarke, D. R.; Lange, F. E. *J. Am. Ceram. Soc.* **1997**, *80*, 575-583.
[6] Israelachvili, J. N. *Intermolecular and Surface Forces*; Academic Press: San Diego, 1991.
[7] Hough, D. B.; White, L. R. *Adv. Colloid Interfac.* **1980**, 14, 3-41.
[8] Kiefer, J. E.; Parsegian, V. A.; Weiss, G. H. *J. Colloid Interf. Sci* **1975**, *51*, 543-546.
[9] Subramanian, V.; Ducker, W. *J. Phys. Chem. B* **2001**, *105*, 1389-1402.
[10] Healy, T. W.; Somasundaran, P.; Fuerstenau, D. W. *Int. J. Miner. Process.* **2003**, *72*, 3-10.
[11] Somasund.P; Healy, T. W.; Fuersten.Dw *J. Colloid Interf. Sci.* **1966**, *22*, 599- 603.
[12] Patel, S. S.; Tirrell, M. *Annu. Rev. Phys. Chem.* **1989**, *40*, 597-635.
[13] Russel, W. B.; Saville, D. A.; Schowalter, W. R. *Colloidal Dispersions*; Cambridge University Press, 1989; Vol. Chapter 6.
[14] Fleer., G. J.; Cohen Stuart, M. A.; Scheutjens, J. M. H. M.; Cos grove, T.; Vincent, B. *Polymers at Interfaces*; Chapman and Hall, 1993; Vol. 301-318; 449-453.
[15] Tirrell, M.; Levicky, R. **1997**, *2*, 668-672.
[16] Milner, S. T. *Science* **1991**, *251*, 905-914.
[17] de Gennes, P. G. *Adv. Colloid Interf.*. **1987**, *27*, 189.
[18] de Laat, A. W. M.; Schoo, H. F. M. *J.Colloid Interf. Sci.* **1997**, *191*, 416-423.
[19] Orth, J.; Meyer, W. H.; Bellmann, C.; Wegner, G. *Acta Polym.* **1997**, *48*, 490-501.
[20] Guzonas, D.; Hair, M. L.; Cosgrove, T. *Macromolecules* **1992**, *25*, 2777-2779.
[21] Bevan, M. A.; Scales, P. J. *Langmuir* **2002**, *18*, 1474-1484.
[22] Wu, D. T.; Yokoyama, A.; Setterquist, R. L. *Polym. J.* **1991**, *23*, 709-714.
[23] Schillen, K.; Claesson, P. M.; Malmsten, M.; Linse, P.; Booth, C. *J. Phys. Chem. B.* **1997**, *101*, 4238 - 4252.
[24] Claesson, P. M. In *Colloid Polymer Interactions*; Farinato, R. S., Dubin, P. L., Eds.; Wiley: New York, 1999.
[25] Butt, H.-J.; Kappl, M.; Mueller, H.; Raitereri, R.; Meyer, W.; Ruhe, J. *Langmuir* **1999**, *15*, 2559-2565.
[26] Palmqvist, L. M.; Lange, F. F.; Sigmund, W.; Sindel, J. *J. Am. Ceram. Soc.* **2000**, *83*, 1585-1591.
[27] Cappello, J.; Crissman, J.; Dorman, M.; Mikolajczak, M.; Textor, G.; Marquet, M.; Ferrari, F. *Biotechnol. Progr.* **1990**, *6*, 198-202.
[28] Barron, A. E.; Zuckermann, R. N. *Curr. Opin. Chem. Biol* **1990**, *3*, 681-687.
[29] McGrath, K. P.; Tirrell, D. A.; Kawai, M.; Mason, T. L.; Fournier, M. *Biotechnol Progr.* **1990**, *6*, 188-192.
[30] van Hest, J. C. M.; Tirrell, D. A. *Chem. Commun.* **2001**, 1897-1904.
[31] Deming, T. J. *Adv. Mater.* **1997**, *9*, 299-311.
[32] Whaley, S. R.; English, D. S.; Hu, E. L.; Barbara, P. F.; Belcher, A. M. *Nature* **2000**, *405*, 665-668.
[33] Yamakawa, H. *Modern Theory of Polymer Solutions*; Harper & Row: New York, 1971.
[34] Mattice, W. L.; Mandelkern, L. *J. Am. Chem. Soc.* **1971**, *93*, 1769.
[35] Krsmanovic, J.; *Ph.D. thesis*, Virginia Tech, 2003.
[36] Lu, Z.; Diblasio-Smith, E. A.; Grant, K. L.; Warne, N. W.; LaVallie, E. R.; Collins-Racie, L. A.; Follettie, M. T.; Williamson, M. J.; McCoy, J. M. *J. Biol. Chem.* **1996**, *271*, 5059-5065.
[37] Lavallie, E. R.; DiBlasio, E. A.; Kovacic, S.; Grant, K. L.; Schendel, P. F.; McCoy, J. M. *Bio-Technol.* **1993**, *11*, 187-193.
[38] Protein Data Base
[39] Holmgren, A.; Soderberg, B.; Eklund, H.; Branden, C. I. *Proc. Natl. Acad. Sci.* **1975**, *72*, 2305-2309.
[40] Pan, Z.; Somasundaran, P.; Senak, L. *ACS Sym. Ser.* **2004**, *878*, 185-204.
[41] Baklouti, S.; Ben Romdhane, M. R.; Boufi, S.; Pagnoux, C.; Chartier, T.; Baumard, J. F. *J. Eur Ceram. Soc.* **2003**, *23*, 905-911.
[42] Ishiduki, K.; Esumi, K. *Langmuir* **1997**, *13*, 1587-1591.
[43] Tada, H.; Saito, Y.; Hyodo, M. *Shikizai Kyokaishi* **1992**, *65*, 671-675.
[44] Cesarano, J.; Aksay, I. A.; Bleier, A. *J. Am. Ceram. Soc.* **1988**, *71*, 250.

[45] Cesarano, J.; Aksay, I. A. *J. Am. Ceram. Soc.* **1988**, *71*, 1062.
[46] Zaman, A. A.; Tsuchiya, R.; Moudgil, B. M. *J. Colloid Interf. Sci.* **2002**, *256*, 73-78.
[47] Reynolds, J. A.; Tanford, C. *Proc. Natl. Acad. Sci.* **1970**, *66*, 1002-1007.
[48] Stryer, L. *Biochemistry*; 4th ed.; W.H. Freeman and Company: New York, 1995.
[49] Derjaguin, B. V. *Kolloid Z.* **1934**, *69*, 155-164 See also Hunter, R. J. Foundations of Colloid Science, Vol. I; Oxford Science Press, Oxford, 1987.
[50] Horn, R. G.; Clarke, D. R.; Clarkeson, M. T. *J. Mater. Res.* **1988**, *3*, 413-416.
[51] Franks, G. V.; Meagher, L. *Colloid Surface A* **2003**, *214*, 99-110.
[52] Sambrook , J.; Fritsch, E. F.; Maniatis, T. "Molecular Cloning: A Laboratory Manual. Cold Spring Harbor Laboratory Press: Cold Spring Harbor N. Y.," 1992.
[53] Ausubel, F. M. *Current Protocols in Molecular Biology.*; J. Wiley: New York, 1997.
[54] Hochstrasser, D. F.; Patchornik, A.; Merril, C. R. *Anal. Biochem.* **1988**, *173*, 424- 435.
[55] Canova-Davis, E.; Eng, M.; Mukku, V.; Reifsnyder, D. H.; Olson, C. V.; Ling, V. T. *Biochem. J.* **1992**, *278*, 207-213.
[56] Bornstein, P.; Balian, G. *Method. Enzymol.* **1977**, *47*, 132-145.
[57] Gill, S. C.; Von Hippel, P. H. *Anal. Biochem.* **1989**, *182*, 319-326.
[58] Beaglehole, D. *Physica A* **1980**, *100B*, 163.
[59] Palik, E. D. *Handbook of Optical Constants of Solids*; Academic Press: New York, 1985.
[60] Beaglehole, D.; Christenson, H. K. *J. Phys. Chem.* **1992**, *96*, 2295.
[61] Arwin, H. *Appl. Spectrosc.* **1986**, *40*, 313-318.
[62] Ball, V.; Ramsden, J. J. *Biopolymers* **1998**, *46*, 489-492.
[63] Jönsson, U.; Malmqvist, M.; Rönnberg, I. *J. Colloid Interf. Sci.* **1985**, *103*, 360-372.
[64] Peters, T. Advances in Protein Chemistry **1985**, 37, 161-245.
[65] Ivarsson, B. A.; Hegg, P. O.; Lundstrom, K. I.; Jonsson, U. *Colloid and Surface* **1985**, *13*, 169-192.
[66] Ducker, W.; Senden, T. J.; Pashley, R. M. *Langmuir* **1992**, *8*, 1831-1836.
[67] Cleveland, J. P.; Manne, S.; Bocek, D.; Hansma, P. K. *Rev. Sci. Instrum.* **1993**, *64*, 403-406.
[68] Ivanova, M. A.; Arutyunyan, A. V.; Lomakin, A. V.; Noskin, V. A. *Appl. Optics* **1997**, *36*, 7657-7663.